

Coal-Seq II Consortium

Technical Progress Report

Period from January 1, 2006 through March 31, 2006

Summary

- During the last period BP has joined the consortium, and Schlumberger has verbally agreed to join. The consortium is now 80% subscribed. New member prospects include ConocoPhillips, ExxonMobil, El Paso, EnCana and Halliburton.
- Unique visitors to the project website were 320, 290, and 348 for January, February, and March respectively.
- Planning for the Coal-Seq V Forum was initiated, anticipated to be November 8th & 9th in the Houston area.
- Received notice that abstract for GHGT-8 conference was accepted.
- Progress reports for each subcontractor, plus a financial status report, are provided in the attachments.

Attachments

- Quarterly Progress Report – Electrochemical Systems, Inc.
- Quarterly Progress Report – Oklahoma State University
- Quarterly Progress Report – Southern Illinois University
- Financial Status Report

Quarterly Progress Report

Electrochemical Systems, Inc.

Period from January 1, 2006 through March 31, 2006


Task 1: Develop FORTRAN Code to Calculate the Densities and Partial Fugacities of Mixed CO₂-CH₄ Gases in Subsurface Coalbeds

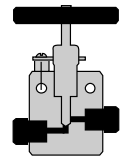
Significant progress was made this quarter in procuring the remaining equipment required to build the gas densimeter. Listed below are specifications for a desktop computer and National Instruments Corporation modules that will be used to gather and store the experimental data we obtain. A LabView™ computer program to receive the output signals from our Paroscientific pressure transducers and YSI thermistors is now nearly complete. In a separate but related activity, gas delivery and vacuum manifolds were designed and major components purchased. Finally, design work was completed and engineering drawings were prepared for: (1) a safety/thermal shield for the densimeter tank, and (2) mounting brackets for an in-tank gas manifold. These components will be fabricated and installed during the next quarter.

Equipment Required to Construct the Densimeter Apparatus

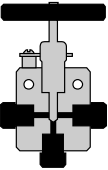
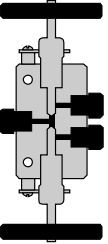
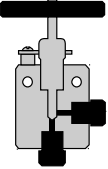
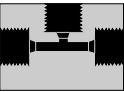
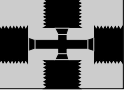
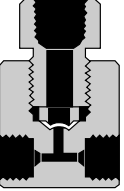



The table below lists the components of the densimeter apparatus that have been received or ordered.

Components Ordered and Received During this Quarter


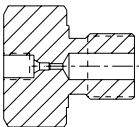
Mfg	Part No.	Description	Qty	\$/each	\$ cost **	
YSI	031-46046-4.5-RTS4-180-ST-1/8 NPT	YSI thermistor	6	\$310.00	\$2032.05	

Mfg/ Part No	Description	Qty	\$/each	\$/total	Use	Diagram Ref #	
HIP 15-11AF1	2-way straight valve	12	\$76.10	\$913.20	H ₂ O-Bath+Manifold	1, 3, 4, 5, 6, 7, 8, 10, 11, 13, and [4]	



15-14AF1	3-way, 1 pressure connection valve	11	\$81.10	\$892.10	H ₂ O-Bath+Manifold	2, 9, 12, [5]	
15-15AF1	3-way, 2-stem connection valve	2	\$143.00	\$286.00	Manifold		
15-12AF1	2wayangle	3	\$76.70	\$230.10	CFWA cylinder	[5]	
15-23AF1	Tee	2	\$33.00	\$66.00	Manifold		
15-24AF1	Cross	2	\$42.00	\$84.00	Bath		
15-63AF1	Safety Head	1	\$101.00	\$101.00	Manifold		
RD-5000	Rupture Disc 5kpsi	1	\$24.45	\$24.45	Manifold		
15-9A1-030	1/16-in OD tube x 0.030-in ID high pressure tubing	40 ft	\$3.30/ft	\$132.00	Bath+Manifold		
15-2A1	Taper Seal Connection Sleeve	36	\$1.95	\$70.20	Bath+Manifold		
15-2AM1	Taper Seal Gland Nut	12	\$3.60	\$43.20	Bath+Manifold		



15-7AM1	Taper Seal Plug	12	\$3.10	\$37.20	Bath+Manifold		
211377 ASY	AF1 to Male 5/8-18 Thread Adapter	3	\$130.00	\$390.00	CFWA cylinder		
Total Cost Items Received				\$5301.50			

Components Ordered

Dell Computer							
Dimension B110	CPU	1	\$648.00	\$648.00	Data acquisition		
UltraSharp 2005FPW	Monitor, 20.1-inch Flat Panel LCD	1	\$423.20	\$423.20	Data acquisition		
National Instruments	NI PCI-8430/4, 4-Port RS-232 High Baud Interface	1	\$445.00	\$445.00	Data acquisition (pressure transmitter interface)		
778979-01							
182845-01	NI S8 Serial Cable, 10Pos Modular Plug to DB-9, 1 meter long (non isolated)	4	\$25.00	\$100.00	Data acquisition (pressure transmitter interface)		
777789-01	NI PCI-4351, High-Precision Temperature & Voltage Logger	1	\$795.00	\$795.00	Data acquisition (thermistor sensor interface)		
182419C-02	NI SH6868 Shielded Cable Assembly, 2 meters long	1	\$150.00	\$150.00	Data acquisition (thermistor sensor interface)		
776844-01	NI SCB-68, Noise Rejecting, Shielded I/O Connector Block	1	\$295.00	\$295.00	Data acquisition (thermistor sensor interface)		
Programmer	LabView Programming	29 hr	\$70.00/hr	\$2030.00 Est.	Data acquisition		
Misc.							
A2N209-25-T	Belkin Pro Series Serial DB9m to DB9F extension 25 ft cable	4	\$14.74	\$58.96	Data Acquisition (pressure transmitter signal)		





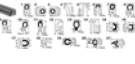
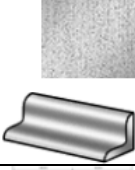






ISOBAR8UL TRA	Tripp Lite Isobar 8 Ultra Surge Protector	1	\$59.98	\$59.98	Data Acquisition		
Total Cost Items Ordered				\$5005.14			

Components to be Ordered


Mfg/ Part No	Description	Qty	\$/each	\$/total	Use	Diagram Ref #	
Swagelok SS-T6-S-065-20	Stainless steel tubing, 3/8-in OD x 0.065-in wall x 40 ft	40 ft	\$3.69	\$147.60	Gas Booster and Vacuum manifolds		
Swagelok SS-RL4S8	Low pressure relief valve (10-20 psi)	1	\$237.10	\$237.10	Vacuum manifold safety system		
Swagelok SS-6P6T	Plug valve, Quarter-Turn Instrument Plug Valve, 3/8 in. Swagelok Tube Fitting, 6.4 Cv	3	\$76.30	\$228.90	Gas Booster and Vacuum manifolds		
Swagelok SS-8P6T2	Plug valve, Quarter-Turn Instrument Plug Valve, 1/2 in. Male NPT, 2.4 Cv	2	\$78.80	\$157.60	Control high pressure air flow to gas booster pump		
Swagelok SS-811-PC-6	Reducing port connector, 1/2 x 3/8	1	\$10.50	\$10.50	Connect vacuum manifold to relief valve		
Swagelok SS-600-1-4	Male connector 3/8-in OD tube to 1/4-in Male NPT	1	\$8.30	\$8.30	Connect gas manifold to gas booster pump		
Swagelok SS-810-1-4	Male connector 1/2-in OD tube to 1/4-in Male NPT	1	\$12.00	\$12.00	Connect compressed air line to gas booster pump		
Matheson	Manual flow control valve	2	\$175	\$350.00	Flow control from reservoir gas cylinders		



Teledyne Hastings VT6A	Thermocouple Vacuum Gauge 0-1000 mTorr, with 0-1 VDC output	1	\$573.00	\$573.00	Measure pressure in evacuated densimeter components	
Teledyne Hastings DV6M	Thermocouple Vacuum Gauge Sensor 0-1000 mTorr range	1	\$61.00	\$61.00	Measure pressure in evacuated densimeter components	
Teledyne Hastings DB20	NIST Reference Tube Thermocouple Vacuum Gauge Sensor 10 mTorr standard	1	\$325.00	\$325.00	Measure pressure in evacuated densimeter components	
LEXAN® Polycarbonate Sheet	Lexan® polycarbonate sheet ¼-in nominal x 48-in x 96-in	1	\$155.00	\$155.00	Safety and thermal shielding for bath tank	
Safety/ Thermal Shield Fabrication	Custom fabricated Lexan® polycarbonate sheet Densimeter bath cover	1	Design submitted for bid		Safety and thermal shielding for bath tank	
Safety/ Thermal Shield Fabrication	McMaster Carr 1120A412 Push-on edge-trim rubber seal	25 ft	\$1.18/ft	\$29.50	Safety and thermal shielding for bath tank	
90° Angle Stock	1-in x 1-in x 3/16-in, 304 stainless steel	8 ft	\$8.00/ft	\$64.00	Bath tank safety/thermal shielding support	
Safety/ Thermal Shield Support Fabrication	Custom fabricated stainless steel supports for polycarbonate sheet Densimeter bath cover		Design submitted for bid		Safety and thermal shielding for densimeter bath tank	
90° Angle Stock	2-in x 4-in x 1/8-in, 304 stainless steel (custom fabrication from stainless steel sheet)	8 ft	\$13.75/ft	\$110.00	Bath tank, valve mounting brackets	
Valve Support Brackets Fabrication	Custom fabricated stainless steel brackets for mounting in-tank densimeter valves		Design submitted for bid		In-tank densimeter valve manifold	
25 Custom Clips	Custom fabricated stainless steel clips for supporting polycarbonate sheet safety/thermal shield		Design submitted for bid		Support safety and thermal shielding in densimeter bath tank	
Quincy QTH-5-80	Quincy 2-stage reciprocating air compressor. 1q7.2 CFM @ 175 psi; 5 HP, 80 gal horizontal tank; 230VAC/3phase/60Hz	1	\$1658.00	\$1658.00	Air compressor used to drive gas booster (Note: cost sharing may reduce the project cost of this equipment)	



	Installation of Air compressor	8 hr	\$70.00/hr	\$560.00			

Grainger 4Z899	Heavy Duty Multi Purpose Rubber Air Hose, Inside Diameter 3/8 Inch, OD 0.687 Inch, Fitting Size 3/8 NPT, Pressure Range 250 PSI, Color Red, Length 50 Feet, Coupled Assembly	1	\$41.25	\$41.25	Supply line to connect air compressor with gas booster pump		
Total Cost Items to be Ordered [Excluding fabrication]				\$ 4728.75			

\$ cost ** Does not include taxes and shipping charges

Task 2: Develop FORTRAN Code to Numerically Represent Bi-Directional CO₂-CH₄ Gas Diffusion in Microporous Coal, and “Free Flow” of Mixed CO₂-CH₄ Gas Through Macropores and Cleats

The following document was written this quarter:

Title: Compressible Fluid Flow in Porous Media. Author: Simon L. Marshall. Length: 13 pages.



Compressible Fluid Flow in Porous Media

Introduction

The calculation of the rate of gas flow is of central importance in the simulation of carbon dioxide enhanced coalbed methane recovery. In terms of the multicomponent mass transfer problem considered in earlier work, the pressure distribution and the gas flow that it induces provides a reference velocity with respect to which the diffusive fluxes of the gas-phase components are defined. The purpose of the following discussion is not only to identify methods by which the gas-flow problem can be solved, but also to bring to light the simplifying assumptions inherent in the various theoretical treatments, and to identify the corresponding requirements that these impose on the equation of state describing the equilibrium fluid properties. The significance of these assumptions is best illustrated with initial reference to well-known steady flow equations applicable to simple geometries. The more general diffusivity equation for the pressure is then introduced, and the relative merits of several methods for reducing this nonlinear partial differential equation to the form of the heat-conduction or (Fickian) diffusion equation, thereby rendering it more amenable to analytical or numerical solution, are discussed.

Darcy's Law and its Integrated Forms

Theoretical models for oil and gas fields are almost always based on Darcy's Law for flow of a fluid through a porous medium. For one-dimensional flow this assumes the form

$$u = -\frac{K}{\mu} \frac{dp}{dx},$$

where u is the superficial fluid velocity, μ is the viscosity, p is the pressure, and K is the permeability. The fluid velocity can itself be written as

$$u = \frac{Q}{A}$$

where Q is a volumetric flow rate (m^3s^{-1}) and A is an area (m^2) perpendicular to the direction of the flow. Since in the SI system, the pressure and viscosity have the respective dimensions of Pa and Pa s, it follows that the permeability must have dimensions of length squared (m^2). In the oil and gas industry, however, the permeability is expressed in darcy (d). A



medium with a permeability of one darcy supports a flow rate of $1 \text{ cm}\cdot\text{s}^{-1}$ of a fluid with viscosity 1 centipoise (cP) subjected to a pressure gradient of $1 \text{ atm}\cdot\text{cm}^{-1}$. Making use of the conversion factors for pressure ($\text{atm} = 101325 \text{ Pa}$), viscosity ($\text{cp} = 10^{-3} \text{ Pa}\cdot\text{s}$), and length ($\text{cm} = 10^{-2} \text{ m}$), the appropriate conversion factor is found to be

$$d = \frac{(10^{-3} \text{ Pa}\cdot\text{s})(10^{-2} \text{ m})(10^{-2} \text{ m}\cdot\text{s}^{-1})}{(1.01325 \times 10^5 \text{ Pa})} = 0.986923 \times 10^{-12} \text{ m}^2,$$

or about $1 \mu\text{m}^2$. More generally, Darcy's Law is written in vector form as

$$\mathbf{u} = -\frac{1}{\mu}\mathbf{K}\nabla p,$$

where \mathbf{K} is the permeability tensor. The permeability tensor is symmetric, and the flow can always be referred to a coordinate system coinciding with the principal axes of the tensor (so that the off-diagonal elements vanish.) Anisotropic permeability is encountered in sedimentary formations, in which the horizontal permeability is often greater than the vertical permeability.

Under steady-state conditions, Darcy's Law can be integrated for various geometries to give the flow rates corresponding to a specific pressure drop. Thus, if the density and viscosity are independent of pressure, the simplest case of linear one-dimensional flow gives

$$\int_0^L Q dx = -\frac{KA}{\mu} \int_{p(0)}^{p(L)} dp$$

$$Q = -\frac{kA}{\mu L} [p(L) - p(0)].$$

For flow of an incompressible fluid across a cylindrical surface of height H , the superficial velocity is

$$u = \frac{Q}{2\pi r H} = -\frac{K}{\mu} \frac{dp}{dr},$$

and integration with respect to r between limits R_1 and R_2 ($R_1 < R_2$) gives

$$\frac{Q}{2\pi H} \ln \frac{R_2}{R_1} = -\frac{K}{\mu} [p(R_2) - p(R_1)],$$

or

$$Q = -\frac{2\pi H K}{\mu} \frac{p(R_2) - p(R_1)}{\ln(R_2/R_1)}.$$



For the flow of compressible fluids, it is necessary to introduce the formation volume factor, B , which is the ratio of the volumes of a given quantity of the fluid under reservoir conditions and reference conditions. Using the equation of state $p = zRT/V$ in the form $V = zRT/p$, and assuming that the compressibility factor $z = 1$ at the reference conditions p_0, T_0 , this is

$$B = \frac{V}{V_0} = \frac{p_0 z T}{p T_0}.$$

When the formation volume factor is applied to the volumetric flow rate, the Darcy Law becomes

$$\frac{Q}{A} = -\frac{K}{B\mu} \frac{dp}{dx},$$

and in the integration of this equation, it is necessary to take account of the pressure dependence of z . This can be done in two ways. The simpler and more commonly used approach involves setting the value of z to the average of its values at the upstream and downstream pressures. The more correct alternative procedure is to use a suitable equation of state. For example, if the 2-term volume-explicit virial equation is assumed,

$$z = 1 + \frac{bp}{RT},$$

where b is the second virial coefficient, so that

$$\frac{1}{B} = \frac{T_0}{p_0} \frac{p}{1 + bp/RT}.$$

Integration now results in

$$\int_0^L \frac{Q}{A} dx = -\frac{KT_0}{\mu p_0} \int_{p_0}^{p_L} \frac{p}{1 + bp/RT} dp = \left(\frac{RT}{b}\right)^2 \int_{p_0 b/RT}^{p_L b/RT} \frac{X}{1 + X} dX,$$

and since

$$\left(\frac{RT}{b}\right)^2 \int_{p_0 b/RT}^{p_L b/RT} \frac{X}{1 + X} dX = \left(\frac{RT}{b}\right)^2 \left[\frac{b}{RT}(p_L - p_0) - \ln \frac{1 + p_L b/RT}{1 + p_0 b/RT} \right]$$

one-dimensional linear flow is described by

$$\frac{Q}{A} L = -\frac{KT_0}{\mu p_0} \left(\frac{RT}{b}\right)^2 \left[\frac{b}{RT}(p_L - p_0) - \ln \frac{1 + p_L b/RT}{1 + p_0 b/RT} \right].$$



The special case of an ideal gas is obtained by allowing b to tend to zero, and making use of the power series

$$\frac{1}{1+X} = 1 - X + X^2 - X^3 + \dots, \quad \ln(1+X) = X - \frac{X^2}{2} + \frac{X^3}{3} - \frac{X^4}{4} + \dots,$$

from which it is evident that the terms linear in pressure cancel, leaving

$$\left(\frac{RT}{b}\right)^2 \left[\frac{1}{2} \left(\frac{b}{RT}\right)^2 (p_L^2 - p_0^2) - \frac{1}{3} \left(\frac{b}{RT}\right)^3 (p_L^3 - p_0^3) + \dots \right].$$

Therefore, taking the limit as $b \rightarrow 0$,

$$\lim_{b \rightarrow 0} \left(\frac{RT}{b}\right)^2 \left[\frac{b}{RT} (p_L - p_0) - \ln \frac{1 + p_L b / RT}{1 + p_0 b / RT} \right] = \frac{1}{2} (p_L^2 - p_0^2),$$

so that the ideal-gas flow equation is

$$\frac{Q}{A} L = -\frac{KT_0}{\mu p_0} \frac{1}{2} (p_L^2 - p_0^2).$$

Obviously, the integration on the left-hand side of the Darcy equation could be appropriately modified to give the corresponding result for radial flow.

The Diffusivity Equation

The three essential components needed to describe the flow of a compressible fluid are the velocity, the pressure, and the density. While in principle, these three quantities can be obtained by simultaneous solution of the equation of motion (Darcy's Law), the continuity equation (which expresses the conservation of matter), and the equation of state (relating pressure to the density), in practice it is more convenient to combine them into a single partial differential equation for the pressure. This is the so-called Diffusivity Equation, the following derivation of which is based on the discussions presented by Amanat U. Chaudhry, "Gas Well Testing Handbook", Amsterdam: Elsevier (2003); and Chi U. Ikoku, "Natural Gas Reservoir Engineering", New York: Wiley (1984).

The continuity equation appropriate to flow through a medium of porosity ϕ is

$$\nabla \cdot (\rho \mathbf{u}) = -\frac{\partial}{\partial t} (\rho \phi),$$



where ρ is the molar density (this is used in preference to the mass density to maintain consistency with the form of most equations of state in common use). If the permeability is isotropic, Darcy's Law gives

$$\mathbf{u} = -\frac{K}{\mu}\nabla p,$$

and when this is substituted into the continuity equation the result is:

$$\nabla \cdot \left(\frac{K\rho}{\mu}\nabla p \right) = \frac{\partial(\rho\phi)}{\partial t}.$$

This can be rewritten entirely in terms of the pressure by making use of the equation of state in the form

$$\rho = \frac{p}{zRT}.$$

The crucial step in this process is the introduction of the isothermal compressibility κ_T

$$\begin{aligned}\kappa_T &= \frac{1}{\rho} \left(\frac{\partial \rho}{\partial p} \right)_T \\ &= \frac{zRT}{p} \frac{\partial}{\partial p} \left(\frac{p}{zRT} \right) = \frac{z}{p} \frac{\partial}{\partial p} \left(\frac{p}{z} \right)\end{aligned}$$

so that

$$\frac{\partial}{\partial p} \left(\frac{p}{z} \right) = \frac{\kappa_T p}{z}.$$

From this result it follows that

$$\nabla \left(\frac{p}{z} \right) = \frac{\partial}{\partial p} \left(\frac{p}{z} \right) \nabla p = \frac{\kappa_T p}{z} \nabla p$$

and

$$\frac{\partial}{\partial t} \left(\frac{p}{z} \right) = \frac{\partial}{\partial p} \left(\frac{p}{z} \right) \frac{\partial p}{\partial t} = \frac{\kappa_T p}{z} \frac{\partial p}{\partial t}.$$

Assuming that the porosity ϕ , permeability K , viscosity μ and temperature T are constant, the left-hand side of the equation becomes

$$\nabla \cdot \left(\frac{K\rho}{\mu}\nabla p \right) = \frac{K}{\mu RT} \nabla \cdot \left(\frac{p}{z}\nabla p \right) = \frac{K}{\mu RT} \left[\frac{p}{z}\nabla^2 p + \nabla \left(\frac{p}{z} \right) \cdot \nabla p \right]$$



$$= \frac{K}{\mu RT} \frac{p}{z} [\nabla^2 p + \kappa_T \nabla p \cdot \nabla p],$$

and the right-hand side becomes

$$\frac{\partial(\rho\phi)}{\partial t} = \frac{p \phi \kappa_T}{z RT} \frac{\partial p}{\partial t}.$$

After cancelation, the partial differential satisfied by the pressure is found to be

$$\frac{\partial p}{\partial t} = \frac{K}{\mu \phi \kappa_T} [\nabla^2 p + \kappa_T \nabla p \cdot \nabla p].$$

This is known as the Diffusivity Equation, since if permeability is expressed in m^2 , viscosity in $\text{Pa}\cdot\text{s}$, and compressibility in Pa^{-1} , the quantity $\eta \equiv \frac{K}{\mu \phi \kappa_T}$ multiplying the bracketed terms on the right-hand side has the dimensions of diffusivity: m^2s^{-1} . If the compressibility is constant and the pressure gradient is sufficiently small for the nonlinear term to be regarded as negligible, the equation for p clearly reduces to the classical diffusion equation.

Analytical Transformation

Most discussions of the diffusivity equation (such as those presented in the two references cited above) are principally concerned with limiting conditions under which the nonlinear squared-gradient term can be neglected and the pressure satisfies the diffusion equation. For a fluid of constant compressibility, it is, however, also possible to remove the nonlinearity by means of a transformation of variables. This involves introduction of the new variable

$$y = \frac{1}{\kappa_T} e^{\kappa_T p}, \quad p = \frac{1}{\kappa_T} \ln(\kappa_T y).$$

which is also seen to possess the same dimensions as pressure. The required derivatives can be obtained by use of the chain rule,

$$\nabla p = \frac{1}{\kappa_T y} \nabla y, \quad \kappa_T (\nabla p)^2 = \frac{1}{\kappa_T y^2} (\nabla y)^2, \quad \nabla^2 p = \frac{1}{\kappa_T y} \nabla^2 y - \frac{1}{\kappa_T y^2} (\nabla y)^2,$$

and

$$\frac{1}{\eta} \frac{\partial p}{\partial t} = \frac{1}{\eta \kappa_T y} \frac{\partial y}{\partial t}.$$



On combining the expressions for each of the pressure derivatives in the diffusivity equation

$$\frac{1}{\eta} \frac{\partial p}{\partial t} = \nabla^2 p + \kappa_T \nabla p \cdot \nabla p,$$

the squared gradient terms cancel, and multiplication of both sides by $\kappa_T \eta$ leaves the equation

$$\frac{1}{\eta} \frac{\partial y}{\partial t} = \nabla^2 y,$$

as required. Thus, if the hydraulic diffusivity η is constant (as it is to a good approximation for liquids), the transient pressure in a slightly-compressible fluid in a porous medium can be determined by any of the classical methods (such as Laplace Transformation) for solving transient linear heat-conduction or diffusion problems.

Pseudopressure Equation

The conditions under which the nonlinearities in the diffusivity equation can be removed - either by the above analytical transformation or by simply neglecting the squared-gradient term - are most unlikely to be satisfied for the flow of gases through porous media. It is, however, possible to reduce the diffusivity equation to a diffusion equation with a variable diffusivity, by introducing the pseudopressure, defined by

$$\psi = 2 \int_{p_0}^p \frac{p}{\mu z} dp,$$

for which

$$\frac{\partial \psi}{\partial p} = \frac{2p}{\mu z}.$$

The derivatives of ψ can then be related to those of p by

$$\nabla \psi = \frac{2p}{\mu z} \nabla p, \quad \frac{\partial \psi}{\partial t} = \frac{2p}{\mu z} \frac{\partial p}{\partial t}.$$

Writing the latter relationship in the form

$$\frac{\mu}{2} \frac{\partial \psi}{\partial t} = \frac{p}{z} \frac{\partial p}{\partial t},$$



the right-hand side of the diffusivity equation transforms as follows:

$$\frac{\partial(\rho\phi)}{\partial t} = \frac{\phi}{RT} \frac{\partial}{\partial t} \left(\frac{p}{z} \right) = \frac{\phi\kappa_T p}{RT z} \frac{\partial p}{\partial t} = \frac{\phi\kappa_T \mu}{RT} \frac{\partial \psi}{\partial t}.$$

Making use of the equation of state, the pressure gradient appearing in the left-hand side of the diffusivity equation is

$$\frac{\rho K}{\mu} \nabla p = \frac{K}{RT} \frac{p}{\mu z} \nabla p = \frac{K}{2RT} \nabla \psi,$$

so that

$$\nabla \cdot \left(\frac{K\rho}{\mu} \nabla p \right) = \frac{1}{2RT} \nabla \cdot (K \nabla \psi) = \frac{K}{2RT} \nabla^2 \psi,$$

assuming that the permeability is constant. The equation for the pseudopressure is therefore

$$\frac{\partial \psi}{\partial t} = \frac{K}{\phi\kappa_T \mu} \nabla^2 \psi.$$

The determination of the pseudopressure therefore reduces to the solution of a nonlinear diffusion equation. Although the equation of state does not appear explicitly, it is needed to calculate the isothermal compressibility that appears in the variable diffusivity.

Useful insights into the relation between the pseudopressure formulation and the steady-flow equations first considered can be derived by considering the particular case of a real gas described by the volume-explicit two-term virial equation, for which the pseudopressure can be calculated thus:

$$\psi = 2 \int_{p_0}^p \frac{p}{\mu z} dp = \frac{2}{\mu} \int_{p_0}^p \frac{p}{1 + bp/RT} dp.$$

The integral that appears here is exactly the same as that in the earlier solution of the Darcy equation for such a gas, except that the upper limit is p rather than the upstream pressure p_L . Therefore, for this fluid

$$\psi = \frac{2}{\mu} \left(\frac{RT}{b} \right)^2 \left[\frac{b}{RT} (p - p_0) - \ln \frac{1 + bp/RT}{1 + bp_0/RT} \right].$$

In these terms, the steady-flow expression derived earlier can be written more succinctly as

$$\frac{Q}{A} = - \frac{KT_0}{\mu p_0} \frac{\psi(L) - \psi(0)}{L} = - \frac{KT_0}{\mu p_0} \frac{\Delta \psi}{L},$$



which follows more directly by seeking the appropriate solution of the equation

$$\nabla^2 \psi \equiv \frac{d^2 \psi}{dx^2} = 0$$

in the interval $x \in [0, L]$.

The equation of state used in this particular example is sufficiently simple for the pseudopressure integral to be evaluated analytically. Calculation of the pseudopressure from pressure for more complicated volume- or pressure-explicit equations of state would in general require numerical quadratures. This process would be considerably more complicated for pressure-explicit equations, considering that the compressibility factor is defined implicitly, and would have to be determined (usually by iteration) for each pressure abscissa used in the integration rule. Moreover, incorporation of the pressure-dependence of the viscosity according to the Dean-Stiel procedure also involves evaluation of an equation of state. On the other hand, the reverse calculation of pressure from the pseudopressure would be simpler for pressure-explicit equations of state, since recovery of the actual pressure from the pseudopressure could be achieved by differentiation according to

$$p = \frac{\mu z}{2} \frac{\partial \psi}{\partial p}.$$

The pressure-derivative of ψ required for this purpose could in principle be obtained by use of an empirical polynomial expression for ψ as a function of p and composition, constructed in advance for the required equation of state. In contrast, the reverse calculation for volume-explicit equations of state, would involve iterative numerical solution of a nonlinear equation in the single variable p , which can easily be achieved.

The solution of the time-dependent equation is considerably complicated by the presence of the variable diffusivity, in that use of implicit finite-difference schemes (which are well known to be inherently more stable than explicit ones) would result in a system of nonlinear algebraic equations that would have to be solved iteratively. On the other hand, these complications vanish in the steady-state limit, in which the pseudopressure satisfies the Laplace equation,

$$\nabla^2 \psi = 0.$$

This can be achieved by any of the main techniques of potential theory, including Fourier series and Green functions. For example, if the injection



and production wells penetrated the entire thickness of the coal seam, the steady-state pseudopressure distribution would consist of a collection of line sources and sinks. If the wells did not penetrate the entire coal seam, the pressure distribution could be constructed by integration of the appropriate Green function for a slab bounded by two parallel planes, along the lengths of the wells. For this purpose, the most convenient representation of the Green function would be as a Fourier-Bessel integral, since the integration with respect to the z -coordinate could be performed explicitly.

Squared-Pressure Equation

Yet another reduction of the diffusivity equation to a diffusion equation is possible if it is assumed that both the compressibility factor and the viscosity are constant; the former could be set equal to its average value over the pressure range of interest. This treatment, which is widely used as the basis for interpreting transient pressure tests of gas wells, starts from the observations that

$$\nabla \left(\frac{p^2}{2} \right) = p \nabla p, \quad \frac{\partial}{\partial t} \left(\frac{p^2}{2} \right) = p \frac{\partial p}{\partial t}$$

and

$$\nabla^2 \left(\frac{p^2}{2} \right) = \nabla \cdot (p \nabla p) = p \nabla^2 p + \nabla p \cdot \nabla p.$$

With the assumptions of constant viscosity and compressibility factor, the diffusivity equation is transformed to

$$\nabla \cdot (p \nabla p) = \frac{\phi \mu}{K} \frac{\partial p}{\partial t},$$

and in view of the above results can be transformed to an equation in p^2 :

$$\nabla^2 \left(\frac{p^2}{2} \right) = \frac{\phi \mu}{K p} \frac{\partial}{\partial t} \left(\frac{p^2}{2} \right).$$

This equation is still nonlinear, in view of the pressure-dependence of the coefficient of $\partial(p^2/2)/\partial t$. It is also evidently inconsistent, since it predicts that all nonideality effects are manifested only under transient conditions. Thus, the steady-state pressure is the solution of

$$\nabla^2 \left(\frac{p^2}{2} \right) = 0,$$



which is the same as for an ideal gas. This is also consistent with the result obtained by the integration of Darcy's Law for flow of an ideal gas. Thus, for one-dimensional linear flow between pressure limits $p(0) = p_0$ and $p(L) = p_L$, the steady-state equation reduces to

$$\frac{d^2}{dx^2} \left(\frac{p^2}{2} \right) = 0,$$

and has a solution proportional to

$$\frac{1}{2L}(p_L^2 - p_0^2).$$

Discussion

From the preceding sections, it is apparent that the least restrictive assumptions on the nature of the fluid are required by the pseudopressure formulation, and the most restrictive by the squared-pressure approach. The analytical transformation of the diffusivity equation is appropriate for flow of a slightly compressible fluid, and as such is not suitable for description of gaseous mixtures, but potentially useful in describing the flow behavior of saline water that might be present in the coal seam.

The diffusion equation satisfied by the pseudopressure is in principle amenable to numerical solution by well-established methods, which can be applied in regions of arbitrary shape. Most of these numerical methods are, however, designed for linear problems in which the diffusivity parameter is independent of the concentration or temperature. The application of such general methods to the present problem would have to be carried out in an iterative manner: starting from an initial guess (in which the hydraulic diffusivity is calculated at the average of the pressure range of interest), the linear problem is solved. A new set of diffusivity values is calculated, corresponding to the pressures calculated in the first pass, and the whole procedure is repeated until successive values of the diffusivity are in satisfactory agreement.

Calculation of the pseudopressure is potentially more complex than the simple form of the defining equation would suggest. Hidden complexities become evident in the calculation of the values of the hydraulic diffusivity for highly-compressible fluids, such as carbon dioxide in the vicinity of its critical temperature. For example, at $100^\circ\text{F} = 310.93\text{ K} = 1.023 T_c$ and $1000\text{ psi} = 6.894\text{ MPa}$, the compressibility of CO_2 is about $1.03 \times 10^{-6}\text{ Pa}^{-1}$,



and the viscosity is approximately $0.0295 \text{ cp} = 2.95 \times 10^{-5} \text{ Pa}\cdot\text{s}$. Therefore, in a formation with a permeability of $1 \text{ md} = 0.986 \times 10^{-15} \text{ m}^2$ and 30% porosity, the hydraulic diffusivity is $\eta=1.08 \times 10^{-4} \text{ m}^2\text{s}^{-1}$. If the length scale (for example, the thickness) of the formation is $L=10 \text{ m}$, this means that the time constant characterizing the transient behavior of the system - at the point where these conditions prevail - is $\tau = L^2/\eta=9.26 \times 10^5\text{s}$ or just over 10 days! Of course, these conditions do *not* prevail throughout the entire system, but this example shows that the time-constants can vary over orders of magnitude if the range of pressure and temperature includes state points at which the compressibility is very large. Thus, if the compressibility were 1000 times smaller, as it might be for a fluid that was far above its critical temperature, the time constant for this hypothetical system would be about 900 s or 15 minutes. Furthermore, the magnitude of these variations could give rise to some convergence difficulties in the numerical scheme suggested above.

Significant differences have been noted between calculated pressure transients obtained from simulators based on the pseudopressure and on squared-pressure formulations. In very interesting work, Beliveau and Fair (Dennis Beliveau and P.S. Fair, "Phase behavior impacts of supercompressible fluids on pressure transient analyses", paper No. SPE 28423, presented at the 69th Annual Technical Conference and Exhibition of the Society of Petroleum Engineers, New Orleans, 1994) calculated pressure transients with gas-well simulators based on the pseudopressure formulation. Their results demonstrated that the 'supercompressibility' characteristic of fluids in the vicinity of vapor-liquid critical points could give rise to pressure transients that would be interpreted quite differently on the basis of other simulation techniques.

The importance of compressibility effects, as demonstrated by the work of Beliveau and Fair (1994), also underscores the need for an equation of state that not only represents the volumetric data correctly, but predicts the correct behavior in the vicinity of the critical point. In this regard, the two-term volume-explicit virial equation used earlier to illustrate the pseudopressure treatment of one-dimensional steady flow is manifestly inadequate. The simplest equations of state that are capable of predicting qualitatively correct vapor-liquid equilibrium behavior are cubic equations of the generalized van der Waals-type:

$$p = \frac{RT}{v - b} - \frac{a}{v^2 + cv + d}$$

in which the parameters a , b , c , and d are all assumed to be functions of tem-



perature and composition. Such equations are very widely used by chemical engineers to represent vapor-liquid equilibrium in nonpolar fluids, such as mixtures of carbon dioxide with light hydrocarbons, but these equations are almost invariably parameterized purely on the basis of vapor-liquid equilibrium data, with little if any use being made of single-phase pressure-density isotherms. Equations of state for gas mixtures should be fitted simultaneously to both types of data. Our preliminary results with multiproperty Generalized Nonlinear Least Squares suggests that the generalized van der Waals cubic possesses sufficient flexibility for this purpose, which appears to contradict the prevailing consensus in the literature.

Summary

- The equation of motion of a compressible fluid in a porous medium can be reduced in several ways to the form of a linear (or quasilinear) diffusion equation. Of these, the pseudopressure equation is the most suitable for application to coalbed methane recovery.
- The pressure-dependence of compressibility and viscosity of gases in the vicinity of the critical point can give rise to large variations in the hydraulic diffusivity.
- Reliable simulations require an equation of state capable of reproducing the form of pressure-density isotherms near the critical point. In this regard, generalized van der Waals-type cubic equations appear to offer better prospects of success than truncated virial equations.



Improved Adsorption Models for Coalbed Methane Production and CO₂ Sequestration

Progress Report

January 1, 2006 to March 31, 2006

K. A. M. Gasem
R. L. Robinson, Jr.
(Principal Investigators)

J. E. Fitzgerald
S.A. Mohammad
J.S. Chen

Oklahoma State University
School of Chemical Engineering
Stillwater, Oklahoma 74078-0537

Prepared for

Advanced Resources International
Houston, Texas 77042

April 20, 2006



Disclaimer

The Principal Investigators agreed to undertake this research on a best effort basis. Neither Oklahoma State University and the Principal Investigators, nor any of their employees, make any warranty, express or implied, or assumes any legal liability or responsibility for the accuracy, completeness, or usefulness of any information, apparatus, product, or process disclosed or represents that its use would not infringe privately owned rights.



Executive Summary

Complementary tasks involving experimental work and model development were undertaken to meet the project objectives. Following is a summary of our accomplishments for this reporting period:

Experimental Work

- An adsorption isotherm was measured for CO₂ on wet Pocahontas coal at a temperature of 328.2 K (131 °F) and pressures to 13.8 MPa (2000 psia). This was a replicate run conducted using an improved experimental design, which resulted in the lowering of experimental uncertainty from 16% to 5% on average. The adsorption measurement was conducted at the equilibrium moisture content of roughly 1%.

At 1000 psia, the adsorption of CO₂ on wet Pocahontas was roughly 21% lower in the amount of gas adsorbed when compared to the adsorption on the dry coal.

- As part of **Task 2** of the experimental program, an adsorption isotherm was also measured for CO₂ on wet activated carbon at a temperature of 328.2 K (131 °F) and pressures to 13.8 MPa (2000 psia). The adsorption data for this isotherm yielded expected uncertainties of 2% on average. The adsorption measurement was conducted at the equilibrium moisture content of 27%.

Adsorption of CO₂ on wet activated carbon exhibited a change in concavity at about 600 psia, and the wet AC adsorption amount approaches that of the dry AC at pressures above 1200 psia. This may be an experimental artifact resulting from uncertainty in the calculated gas density, caused by the presence of water vapor in the CO₂ gas phase. Some experimental evidence suggests that the presence of small concentrations of water in the gas phase increases the CO₂ gas density by as much as 10%. A correction of this magnitude leads to the adsorption on the wet activated carbon becoming lower than the adsorption on the dry activated carbon at pressures higher than 1200 psia.

Currently, there is no equation of state capable of calculating accurately the densities of carbon dioxide – water mixtures at near-critical conditions. The uncertainty could, however, be eliminated by installing a vibrating tube density meter to measure directly the gas density in-situ, thus eliminating the uncertainty introduced in the experimental adsorption results.

Model Development

As part of **Task 2** of the model development, the HS-SLD model was modified to accommodate the modeling of pure-water adsorption. Improvements include (1) improved algorithms to calculate the adsorption behavior, (2) new numerical integration routines to accommodate discontinuities in the local density profile, and (3) accounting



for the dipole moment of water in the fluid-solid potential expression. Each of these items is discussed below.

1. The HS-SLD adsorption model requires a more elaborate algorithm to calculate the adsorption of water, compared to the algorithm currently used for CO₂ methane, nitrogen, and ethane. At experimental and reservoir conditions, the latter four coalbed gases are substantially above their critical temperatures (supercritical gases). In contrast, water is well below its critical temperature (subcritical fluid). An improved algorithm was developed to address the computational difficulties that arise when dealing with subcritical fluids such as water, which lead to the existence of multiple solutions for the equilibrium criterion relationship (equal chemical potentials). The newly-developed algorithm ensures that all solutions are found, and that the correct solution is implemented in calculating the amount of water adsorbed.
2. The local-density profile depicts how the density of adsorbed fluid varies with distance from the adsorbent surface. This profile is an ensemble of all the local density solutions obtained from the equilibrium criterion relationship. For subcritical fluids, this profile may have discontinuities at certain positions in the profile. The positions of these discontinuities are dependent on temperature, pressure, and the values of model parameters. Such discontinuities cause problems with the currently-used techniques of numerical integration that are used to determine the total amount adsorbed. As a result the calculated adsorption isotherms appear anomalously “jagged” when plotted versus pressure. The new numerical integration routine was developed to alleviate this problem.
3. Water has a significant dipole moment in comparison with the coalbed gases. This dipole moment already is accounted for (within the HS-EOS) in the expression that describes how water molecules interact with each other within the pore slit. However, the 10⁻⁴ potential currently used to describe interactions between the water molecules and the adsorbent surface accounts only for repulsive and van der Waals-type interactions; it does not explicitly take into account the effects of a dipole moment. An additional term was added to the 10⁻⁴ potential to account for the dipole moment of water. Results indicate that this dipole-surface interaction term has a significant effect on the water adsorption capacity. This is relevant for coal characterization because the equilibrium moisture contents of coals can vary widely.

Using the improved algorithm outlined above, the HS-SLD model can represent a range of moisture contents found for various coals; i.e., the model can describe the amount of water adsorbed on each coal.



QUARTERLY REPORT: JANUARY-MARCH 2006
SOUTHERN ILLINOIS UNIVERSITY

PI: S. Harpalani, SIU

Work Completed During the Quarter

Permeability Measurement: Installation of the circumferential extensometer in the triaxial cell was completed. Operational training by the manufacturer, MTS, was completed. Since coal core of suitable diameter was not available, a trial run was carried out using a sandstone core prepared in the SIU specimen preparation laboratory. The triaxial cell base, along with perforated steel disks, core, and extensometer, was assembled. This is shown in Figure 1. Errors in axial and confining stress values were fixed. The sandstone test was performed by applying an axial stress of 630 psi, and a starting horizontal stress of 350 psi. Helium was then passed through the sample at ~300 psi. The objective of the test run was to check the entire experimental setup, and the extensometer's ability to ensure that there was no strain in the horizontal direction. The extensometer was set to zero prior to starting the experiment. With application of applied stresses, and subjecting the sample to gas pressure, there was no strain recorded. Figure 2 shows that the sample was, in fact, under uniaxial strain, that is, there was no lateral strain. The spike between 4 and 12 minutes was the result of applying the axial stress at a very fast pace initially. This will be avoided in the future and the rates of application of stress and gas pressure will be kept low.

Matrix Swelling/Shrinkage Coefficient: The set of experiments involving volumetric strain measurements for step-wise increase in flue gas/CO₂ pressures, and the corresponding step-wise decrease in methane pressure, was completed. The test started with saturating all four samples with methane at 750 psi. After attaining equilibrium, the following different sequences of injection/bleeding were followed:

1. Pure CO₂ was injected into one of the samples. "Simulated" flue gas (13% CO₂ + 87% N₂) was injected into the second sample. This simulated injection of CO₂/flue gas from the commencement of CBM production. The results of volumetric strain for methane/CO₂ and methane/flue gas exchange are shown in Figure 3. The plot shows that the injection of pure CO₂ (in sample 3) results in considerable strain, in excess of three times that induced by methane at 700 psi. The strain induced with injection of simulated flue gas (in sample 4) is negligible, suggesting that swelling behavior with 13% CO₂ is similar to that of pure methane. For pressure steps up to 700 psi, the volume of coal matrix increased by ~0.7% due to methane/CO₂ exchange, and was negligible due to methane/flue gas exchange.
2. The results of methane desorption are shown in Figure 4. The desorption path exhibited (by sample 1) shows some hysteresis in terms of undergoing slightly more shrinkage than the adsorption induced swelling. Injection of flue gas (in sample 2) instead of helium, after the methane partial pressure dropped to ~50% of the starting pressure, induced some swelling. The swelling induced by flue gas injection is the same as the shrinkage induced by bleeding methane, once again, suggesting that 13% CO₂ has the same effect on the volumetric strain as 100% methane.



Prior to starting the second set of experiments to measure volumetric strain, the experimental setup was checked for any errors in the measurement of gas pressure by calibrating the pressure transducers.

Detailed Work Plan: Scott Reeves visited SIU on February 21, 2006. The purpose of the meeting was to roadmap the experimental sequence, experimental conditions, and discuss procurement of coal cores. It was decided to carry out at least four permeability experiments. Each experiment would start with the core being fully saturated with methane at reservoir pressure and temperature. For one experiment, CO₂ will be injected and, for the second, nitrogen will be injected to replicate the two ECBM alternatives for the entire duration of CBM production. For the third and fourth experiments, CO₂/N₂ injection will commence after bleeding methane to reduce the pressure to half of the initial pressure, thus replicating ECBM after partial recovery by pressure depletion. Swelling/shrinkage experiments will be carried out using pure methane, CO₂ and N₂ to estimate the differential swelling, C_k . Only after completing measurement with pure gases, and time permitting, methane will be displaced by injecting N₂ and CO₂ to enable comparison with permeability results. The details of the experimental plan are included in Appendix 1.

With assistance from ARI, BP has agreed to provide coal cores from the San Juan Basin for the experimental work discussed above. Prior to using these cores, an initial set of experiments will be carried out using specimens prepared from a block of coal from Herrin seam in the Illinois Basin.





Figure 1: Triaxial cell base along with perforated steel disks, core and circumferential extensometer.

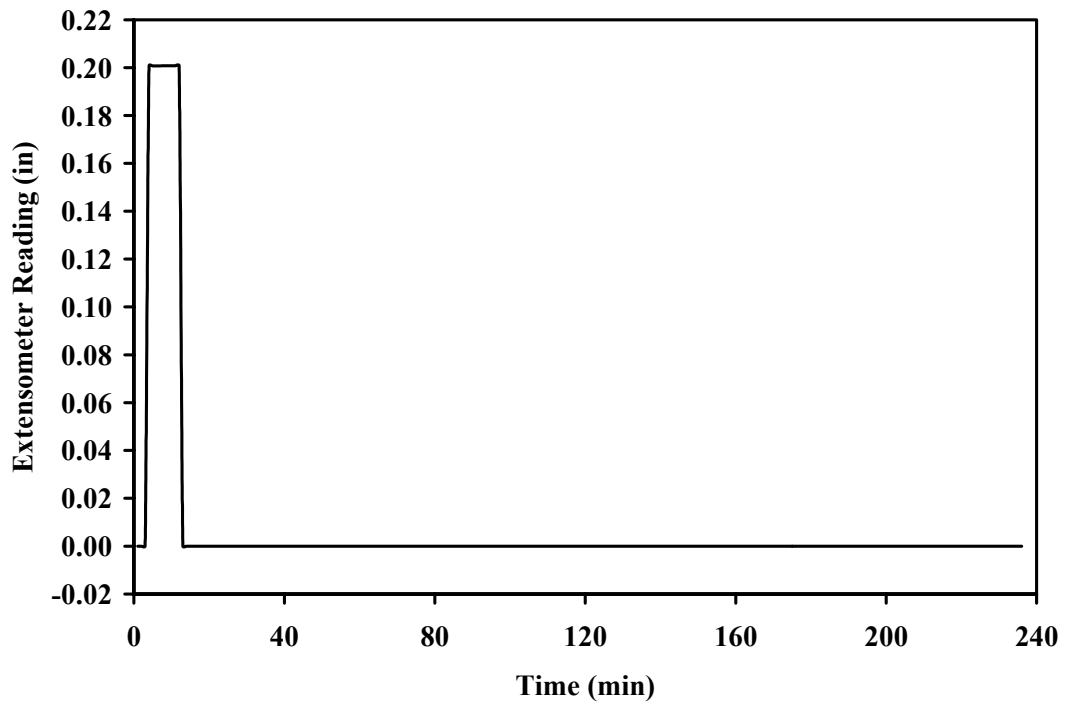


Figure 2: Lateral strain over time.

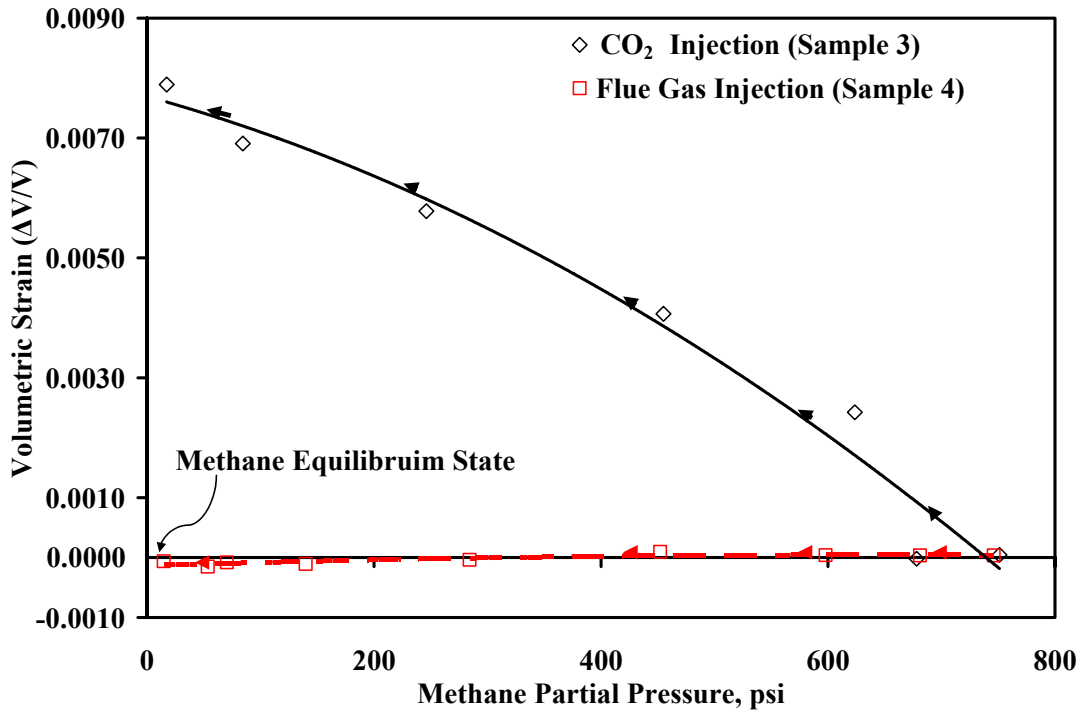


Figure 3: Volumetric strain for methane/CO₂ and methane/flue gas exchange.

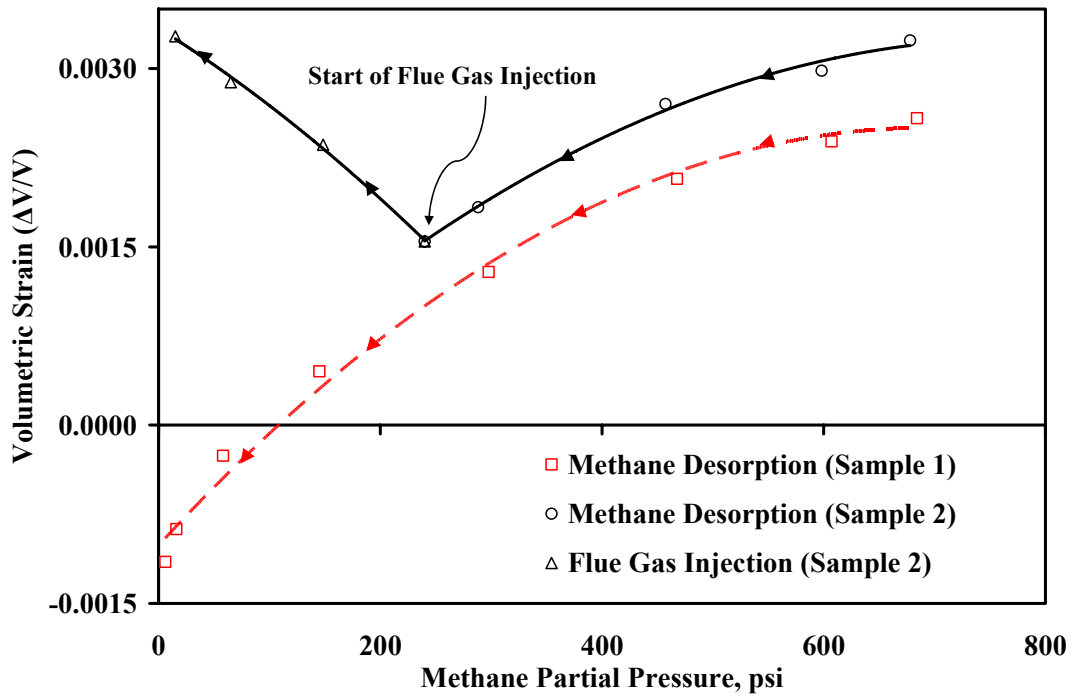


Figure 4: Volumetric strain induced by desorption of methane and injection of flue gas.



APPENDIX 1

DOE/ARI Contract: TASK 2: LABORATORY CORE-FLOOD EXPERIMENTS International ECBM/Sequestration Consortium – Coal-Seq II: Advancing the Science of CO₂ Sequestration in Deep, Unmineable Coal Seams

(Meeting with Scott Reeves: February 21, 2006)

I. PERMEABILITY – FOUR Cores

Experimental Conditions (to be provided by ARI/Consortium)

In situ temperature

In situ gas pressure (Max. Pressure = Virgin condition)

In situ vertical and horizontal stresses (σ_a and σ_h) based on depth

Experimental Sequence

Always start with methane saturated core at P_i (P_{max})

1. Inject CO₂ at P_i and replace methane with CO₂
 2. Inject N₂ at P_i and replace methane with N₂
- { ECBM all the way }

Bleed the core to $\frac{1}{2} P_i$

3. Inject CO₂ at P_i and replace methane with CO₂
 4. Inject N₂ at P_i and replace methane with N₂
- { ECBM after partial depletion }

II. SWELLING/SHRINKAGE (C_k, C_m, C_p)

Objective: Estimate differential swelling, C_k , for CO₂/CH₄ and CH₄/N₂

Experimental Conditions (*in situ* temp and max. pressure)

Experimental Sequence

1. Pure Methane
2. Pure CO₂
3. Pure N₂

Only **after** pure gases, and time permitting, replace methane with N₂ and CO₂ to enable comparison with Permeability results.



**Financial Status Report
March 31, 2006**

	DOE	Industry	Total
Advanced Resources International	20,642	118,295	138,937
Oklahoma State University	107,552	-	107,552
Electrochemical Systems, Inc.	112,519	-	112,519
Southern Illinois University	20,721	-	20,721
Other	11,860	-	11,860
Total	273,296	118,295	391,591
Obligated Funds	750,000	375,000	1,125,000
Remaining Balance	476,704	256,705	733,409
Un-obligated Funds	0.00	375,000	375,000

